Tetrahedron 69 (2013) 9175–9182

Contents lists available at ScienceDirect

Tetrahedron

journal homepage: www.elsevier.com/locate/tet

Metal-free organic dyes with benzothiadiazole as an internal acceptor for dye-sensitized solar cells

Woochul Lee, Ji yeon Seng, Jong-In Hong *

Department of Chemistry, Seoul National University, Seoul 151-747, Republic of Korea

ARTICLE INFO

Article history:
Received 11 June 2013
Received in revised form 26 August 2013
Accepted 30 August 2013
Available online 5 September 2013

Keywords:
Dye-sensitized solar cells (DSCs)
Metal-free organic dyes
Benzothiadiazole
D-A-π-A structures

ABSTRACT

We synthesized three metal-free organic dyes (**H11**–**H13**) consisting of a 3,6-disubstituted carbazole, benzothiadiazole, and cyanoacrylic acid. All the dyes exhibited high molar extinction coefficients and suitable energy levels for electron transfer from the electrolyte to the TiO_2 nanoparticles. Under standard AM 1.5G solar irradiation, the device using dye **H13** with co-adsorbed chenodeoxycholic acid (CDCA) displayed the best performance: an open-circuit voltage (V_{oc}) of 0.71 V, a short-circuit current density (J_{sc}) of 12.69 mA cm^{-2}, a fill factor (FF) of 0.71, and a power conversion efficiency (PCE) of 6.32%. The PCE was ∼79% of that for commercially available N719 cells (8.02%) under the same conditions.

1. Introduction

In recent years, remarkable increases in energy consumption have focused interest on renewable natural energy sources. Among these, solar energy is very attractive as a clean and readily available resource. Since the first report in 1991 by Michael Grätzel et al., dye-sensitized solar cells (DSCs) have received much attention because of their low production costs and relatively high energy conversion efficiencies.[1] Conventional DSCs generally consist of a nanocrystalline titanium oxide (TiO_2) layer, a sensitizer, and an electrolyte. Of these, a highly efficient photosensitizer is an essential factor for the commercialization of DSCs. To date, ruthenium (Ru)-based dyes have achieved high power conversion efficiencies of up to ∼11%[2] under air mass 1.5 global (AM 1.5G) irradiation. However, Ru dyes have some drawbacks, such as low molar extinction coefficients and difficult synthesis and purification. As alternatives to Ru dyes, organic dyes exhibit various advantages, such as high molar extinction coefficients, facile structural modification, relatively low material costs, and environmental friendliness.[3] Remarkable advances have been achieved in metal-free organic dyes,[4] and the highest power conversion efficiency of about 12% has been achieved by using a porphyrin-based dye.[5] As a key factor in the fabrication of highly efficient solar cells, dyes must possess several properties. First, dyes must have a wide absorption overlap with the solar spectrum and exhibit high molar extinction coefficients for efficient light harvesting. Second, appropriate HOMO and LUMO energy levels are required in the dyes for efficient electron injection from the excited dye to the conduction band of TiO_2, and rapid dye regeneration by electron injection into the oxidized dye from the redox couple. Third, the oxidized center in the donor part of the dye must be spatially separated from the TiO_2 film surface to minimize charge recombination between the injected electrons and the resulting oxidized dye.[6]

The general configuration of most reported organic dyes is a D-π-A structure because of its effective photoinduced intramolecular charge transfer (ICT) properties.[7] To improve the efficiency in DSCs, the sensitizers should have good light harvesting ability, which is related to the molecular extinction coefficient and absorption region.[8] In this regard, the highly efficient organic dyes with D-A-π-A structures recently have been described; these incorporate an additional electron-withdrawing moiety, which affords several advantages, such as easy tuning of the molecular energy levels and bathochromic shifts of the absorption region, which improve photovoltaic performance.[9] Typical donor molecular structures are arylamine derivatives, such as triphenylamine or carbazole, which are well known for their strong electron-donating abilities.[10] Benzothiadiazole,[11] benzotriazole,[12] quinoxaline,[13] diketopyrrolopyrrole,[14] and nitro-cyanostilbene[15] are used as internal electron acceptor units. Thiophene or benzene units are often used as π-bridges. Cyanoacrylic acid is commonly used as an acceptor moiety. Phosphinic acid[16] and the rhodanine moiety[17] have also been reported as acceptor units.

In this study, we synthesized and characterized three metal-free organic dyes consisting of a 3,6-bis(triphenylamine)-substituted

---

* Corresponding author. Tel.: +82 2 880 6682; fax: +82 2 889 1568; e-mail address: jihong@snu.ac.kr (J.-I. Hong).

0040-4020/$ – see front matter © 2013 Elsevier Ltd. All rights reserved.
http://dx.doi.org/10.1016/j.tet.2013.08.075

carbazole as an electron donor, benzothiadiazole as an internal acceptor and π-bridge, and cyanoacrylic acid as an anchoring group to bind to TiO_2 nanoparticles. By introducing a star-shaped 3,6-bis(triphenylamine)-substituted carbazole, we were able to build a multi-donor system, which was expected to inhibit the aggregation of the dye on the surface of TiO_2. Especially, a triphenylamine moiety, which was well known for good electron-donating ability as well as hole-transporting property, was incorporated as the donor unit.[18] In addition, a strong electron-withdrawing unit of benzothiadiazole in the π-bridge would result in red-shift of absorption region and facilitating electron transfer from the electron donor to the anchor unit.[8] The photophysical and electrochemical properties and the device performance of H11, H12, and H13 dyes were systemically investigated. All dyes showed high molar extinction coefficients (7×10^4–11×10^4 M^{-1}) and suitable energy levels for electron injection and dye regeneration. The best performance, 6.32%, was achieved by **H13** dye with chenodeoxycholic acid as a co-adsorbent.

2. Results and discussion

2.1. Synthesis

The molecular structures and synthetic procedures for the three dyes are illustrated in Schemes 1 and 2, respectively. 4,7-Di(thiophen-2-yl)benzo[*c*][1,2,5]thiadiazole **1**,[19] 5-(7-(thiophen-2-yl)benzo[*c*][1,2,5]thiadiazol-4-yl)thiophene-2-carbaldehyde **3**,[20] and 3,6-bis-{4-[2-(4-diphenylamino-phenyl)-vinyl]-phenyl}-9*H*-carbazole **7** were synthesized as described in previous reports. The donor moiety was synthesized by the Suzuki reaction, the Heck reaction, and Miyaura borylation.[21] The π-bridges were prepared by the Suzuki reaction. The donor moiety and π-bridge were coupled through the Ullmann or Suzuki reactions. Finally, the Knoevenagel condensation of the formylated compounds **10**, **11**, and **12** with cyanoacetic acid in the presence of piperidine provided dyes **H11**, **H12**, and **H13**, respectively. Precise procedures are described in the Experimental section.

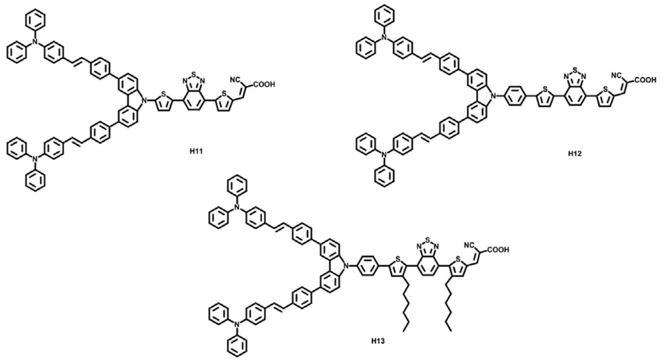

Scheme 1. Molecular structures of **H11**–**H13**.

2.2. Photophysical properties

To investigate the photophysical properties of these dyes, we measured their UV–vis absorption spectra. The absorption spectra of **H11**–**H13** in DMF solution and in TiO_2 films are shown in Fig. 1, and their photophysical data are listed in Table 1. All the dyes exhibited a broad absorption band from 300 to 600 nm corresponding to the π–π* transition (350–450 nm), as well as an intramolecular charge transfer (ICT) band (450–600 nm). H11 and H12 showed similar absorption regions and molar extinction coefficients, which indicates that an additional phenyl unit between carbazole and π-bridge did not contribute to the improvement in light harvesting ability. However, the ICT absorption peak of H13 appears in the blue-shifted region, compared to that of H12, because of a more twisted structure of H13 in the π-bridge. This result is in accordance with the calculated geometry structures of H dyes (Section 2.3). Comparing the absorption spectra of the dyes in solution and as transparent thin films on 4 μm thick TiO_2, significant red-shifts of the absorption onsets were observed, presumably because of the *J*-aggregation of the dye molecules that were anchored to the TiO_2 films.[22]

2.3. Theoretical calculations

To understand the correlation between the molecular structures and their photophysical properties, we performed density functional theory (DFT) calculations at the B3LYP/6-31G* level in the Gaussian 09 package. The frontier molecular orbitals of these molecules are shown in Fig. 2. The HOMOs of the three dyes were delocalized on the donor groups, and the LUMOs were mainly located on the benzothiadiazole, thiophene, and cyanoacrylic acid. This separated electron density extends the absorption onset to the long wavelength region because of the effective ICT. The dihedral angles between the benzothiadiazole and thiophene of **H11** and **H12** were 2.9° and 3.5°, respectively, but the dihedral angle between the benzothiadiazole and hexylthiophene of **H13** was 48.7°. Consequently, **H13**, which has an alkyl chain on thiophene, exhibited a blue-shifted absorption onset because of the twisted structure in the π-bridge.

2.4. Electrochemical properties

The electrochemical properties of these sensitizers were determined by cyclic voltammetry in DMF containing 0.1 M tetrabutylammonium hexafluorophosphate ($TBAPF_6$) as a supporting electrolyte. As shown in Table 1, the oxidation potentials of **H11**, **H12**, and **H13** were 0.90, 0.90, and 0.94 V (vs NHE), respectively. Because the oxidation potentials of these dyes were more positive than the redox potential of I^-/I_3^- (~0.4 V vs NHE), dye regeneration would be a favorable process.[23] The excited state oxidation potentials (E^*_{0-0}) of the dyes were calculated from the equation $E^*_{0-0}=E_{ox}-E_{0-0}$, where the zero–zero excitation energy (E_{0-0}) was derived from the cross point of the normalized absorption and the photoluminescence spectra. The excited state oxidation potentials ($E^*_{0\text{-}0}$) of **H11**, **H12**, and **H13** were −1.46, −1.41, and −1.57 V, respectively. The twisted molecular structure of H13 induced by the two alkyl chains on the π-bridge slightly suppressed the ICT, which resulted in the larger band gap compared to H11 and H12. Because the $E^*_{0\text{-}0}$ values of the dyes were more negative than the conduction band (CB) of TiO_2 (−0.5 V vs NHE), the electron injection process would also be favorable. Thus, these dyes had the requisite energy levels for both efficient electron injection to TiO_2 and the dye regeneration process.

2.5. Photovoltaic performance

DSCs were fabricated with all three dyes and N719 as a reference dye. The liquid electrolyte was composed of 0.6 M 1,2-dimethyl-*n*-propylimidazolium iodide (DMPII), 0.1 M LiI, 0.03 M I_2, and 0.5 M *tert*-butylpyridine (TBP) in acetonitrile/valeronitrile (v/v, 85:15). Current density–voltage curves (*J*–*V* curves, Fig. 3a) and incident photon-to-current conversion efficiencies (IPCE, Fig. 3b) were measured under standard global AM 1.5 solar conditions, and the photovoltaic performance data are displayed in Table 2.

The **H13**-sensitized solar cell showed the best efficiency, with an open-circuit voltage (V_{oc}) of 0.69 V, a short-circuit current density (J_{sc}) of 11.29 mA cm^{-2}, and a fill factor (FF) of 0.68, yielding an overall efficiency (η) of 5.27%. The IPCE intensity usually depends on light

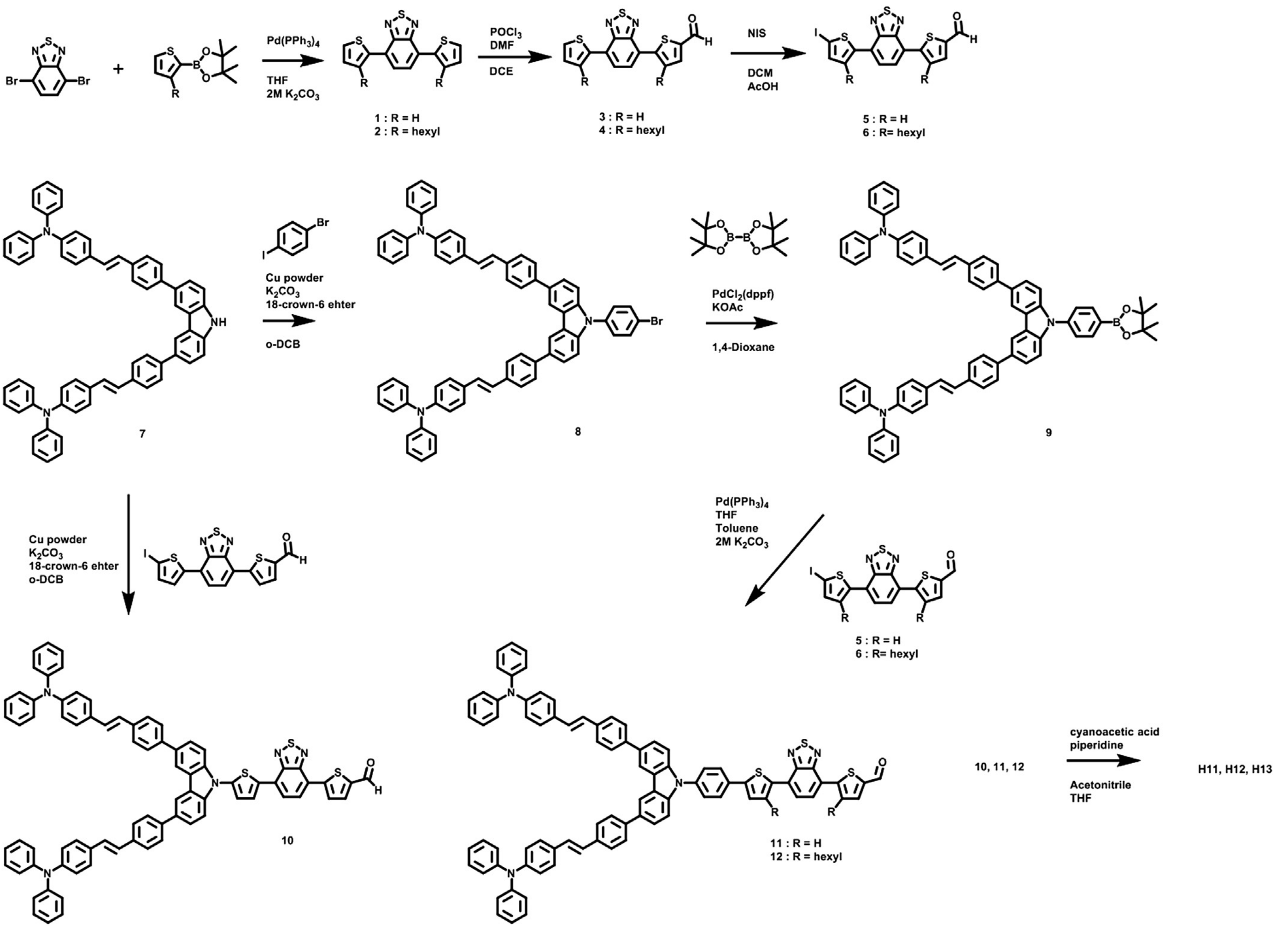

Scheme 2. Synthetic routes of **H11**–**H13**.

absorption as well as photoinduced electron injection into TiO_2 and charge recombination. Generally, the IPCE spectra appeared in the red-shifted region compared to the absorption spectra of dye-adsorbed TiO_2 film because of light scattering in the 400 nm sized TiO_2 layer.[24] As shown in Fig. 3, **H11** and **H12** displayed similar IPCEs, less than 70% in all regions, but **H13** showed a plateau around 400–550 nm and a higher IPCE value, about 70%, than **H11** and **H12**. Although the absorption onset of **H13** was in the shortest region among the three dyes, its photocurrent had the highest value. It is very likely that both the high dye loading amount of H13 and hydrophobic alkyl chains on the π-bridge retarded charge recombination with the oxidized components in the electrolyte (vide infra).

The V_{oc} values of **H11** and **H12** were similar, but that of **H13** was higher, despite the similar oxidation potentials of the three dyes. To discern the reason for the difference in V_{oc} between **H11**–**H13**, we performed electrochemical impedance spectroscopy (EIS) with the **H11**–**H13**-based DSCs. EIS is generally used to investigate the injected electron lifetime in a TiO_2 nanocrystalline layer, which is correlated to the V_{oc} under open-circuit and dark conditions.[25] The three semicircles indicate the resistance of the redox reaction at the platinum counter electrode (first semicircle), the charge recombination at the TiO_2/dye/electrolyte (second semicircle), and the carrier transport by ions within the electrolyte (third semicircle).[26] As shown in Fig. 4a, the radius of the second semicircle in the **H13**-based cell was larger than those of **H11** and **H12**, which means that the charge recombination process was retarded in **H13**-based DSCs. The electron lifetime τ can be obtained from the middle frequency peak in the Bode plot (Fig. 4b) using Eq. 1, where f is the frequency of the peak.

$$\tau = 1/(2\pi f) \tag{1}$$

The injected electron lifetimes of the three **H** dyes were 0.1 (**H11**), 0.1 (**H12**), and 16.5 ms (**H13**), and these results were correlated with the higher V_{oc} value (0.69 V) of **H13**.[27] Thus, the alkyl chains on the π-bridge of **H13** enhanced the photocurrent[28] and suppressed the charge recombination process, which resulted in the improved photovoltaic performance of **H13**.

To enhance the efficiency of the DSCs, chenodeoxycholic acid (CDCA) was co-adsorbed onto the TiO_2 nanoparticles to prevent dye aggregation. As shown in Fig. 5 and Table 2, the J_{sc} of the new device using CDCA increased, and the V_{oc} also slightly increased, yielding an η of 6.33%.

3. Conclusion

We synthesized three metal-free organic dyes consisting of triphenylamine and carbazole as the donor moieties, benzothiadiazole as an internal acceptor and π-bridge, and cyanoacrylic acid as an anchoring group. All three dyes showed the requisite HOMO and LUMO energy levels for dye regeneration and electron injection. The alkyl chains on the π-bridge prevented not only dye aggregation but also charge recombination, leading to high V_{oc} values and high efficiencies. The best efficiency, 6.33%, was

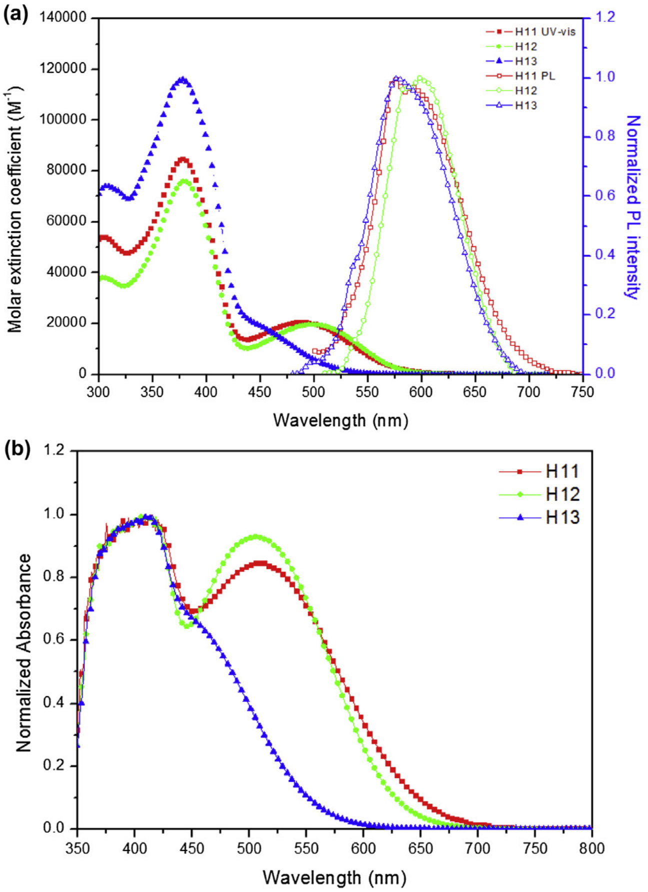

Fig. 1. (a) Absorption and fluorescence spectra of **H11**–**H13** and (b) normalized absorption spectra of dye-loaded TiO_2.

Table 1
Photophysical and electrochemical data for **H11**–**H13**

Dye	λ_{max} (ε)[a]/nm	E_{ox}[b]/V	E_{0-0}[c]/V	E^*_{0-0}[d]/V	HOMO[e]/eV	LUMO[e]/eV	Relative dye loading amount on TiO_2 film
H11	378 (84,980) 488 (20,635)	0.90	2.36	−1.46	−4.90	−3.67	1
H12	379 (76,105) 498 (19,680)	0.90	2.31	−1.41	−4.77	−3.27	1.2
H13	376 (1,16,745)	0.94	2.51	−1.57	−4.74	−3.00	1.3

[a] Maximum absorption wavelengths of dyes in 2.0×10^{-5} M DMF solution.

[b] Measured in DMF with 0.1 M $TBAPF_6$. The oxidation potential was determined from the onset via cyclic voltammetry at a scan rate of 100 mV s^{-1}. Potentials were calibrated against an internal ferrocene/ferrocenium (Fc/Fc^+) standard.

[c] E_{0-0} values were derived from the cross peaks of the normalized absorption spectra and photoluminescence spectra.

[d] Calculated by $E^*_{0-0}=E_{ox.}-E_{0-0}$.

[e] Obtained by DFT calculations using the B3LYP/6-31G* level in the Gaussian 09 package.

obtained with **H13** and 10 mM CDCA, with a V_{oc} of 0.71 V, a J_{sc} of 12.69 mA cm^{-2}, and a FF of 0.71.

4. Experimental

4.1. General information

All organic chemicals were purchased from Aldrich and TCI. Column chromatography was conducted on Merck silica gel 60 (70–230 mesh). All solvents and reagents were commercially available and used without further purification unless otherwise noted. ^1H and ^{13}C NMR spectra were recorded using an Advance 300 MHz Bruker spectrometer. UV–vis spectra were recorded on a Beckman DU 650 spectrophotometer. Mass spectra were obtained using a gas chromatography–mass spectrometry instrument from JEOL (HP 5890 Series II and JMS-AX505WA), and a matrix-assisted laser desorption/ionization time-of-flight (MALDI-TOF) mass spectrometer from Bruker. Fluorescence spectra were recorded on a Jasco FP-7500 spectrophotometer. Cyclic voltammetry (CV) was performed using a CH Instruments 660 Electrochemical Analyzer (CH Instruments, Inc., Texas) with 0.1 M TBAP in DMF at room temperature. CV data were recorded using a Ag/Ag^+ reference electrode (0.1 M $AgNO_3$ in acetonitrile) with a platinum wire counter electrode at a scan rate of 100 mV s^{-1}. The absolute potential was calibrated against the NHE using an internal ferrocene/ferrocenium standard. The theoretical energy levels were obtained by DFT calculations at the B3LYP/6-31G* level in the Gaussian 09 package. The photovoltaic performances of the DSCs were measured using a 1000 W xenon light source, whose power as a Portable Solar Simulator PEC-L01 was calibrated using a KG5-filtered Si reference solar cell. The IPCE spectra for the cells were measured on an IPCE measuring system (PV Measurements). The EIS was measured on a Solar Simulator (Newport) and a potentiostat/galvanostat (Autolab, PGSTAT 302N).

4.2. Synthetic procedures and characterizations

*4.2.1. 4,7-Bis(thiophen-2-yl)benzo[c][1,2,5]thiadiazole (**1**).* This intermediate was prepared as described in a previous report.[29]

*4.2.2. 4,7-Bis(3-hexylthiophen-2-yl)benzo[c][1,2,5]thiadiazole (**2**).* A mixture of 4,7-dibromobenzo[*c*][1,2,5]thiadiazole (475 mg, 1.62 mmol), 2-(3-hexylthiophen-2-yl)-4,4,5,5-tetramethyl-1,3,2-dioxaborolane (1 g, 3.40 mmol), and $Pd(PPh_3)_4$ (187 mg, 0.16 mmol) in THF (20 mL) and 2 M K_2CO_3 (20 mL) was refluxed for 24 h. After cooling to room temperature, the reaction mixture was extracted with dichloromethane (MC), and the organic phase was washed with water, and dried over Na_2SO_4. The solvent was evaporated to give an orange liquid product (580 mg, 77%), which was purified by silica gel column chromatography (eluent; MC/Hexane (Hex)=1:5). ^1H NMR (300 MHz, acetone-d_6): δ (ppm) 7.79 (s, 2H), 7.60–7.58 (d, *J*=5.2 Hz, 2H), 7.18–7.16 (d, *J*=5.2 Hz, 2H), 2.73–2.68 (t, *J*=7.7 Hz, 4H), 1.67–1.57 (m, 4H), 1.27–1.22 (m, 12H), 0.80–0.76 (t, *J*=6.6 Hz, 6H); ^{13}C (75 MHz, $CDCl_3$): δ (ppm) 154.3, 141.7, 132.2, 129.9, 127.5, 125.9, 31.6, 30.7, 29.4, 29.1, 22.6, 14.1; MALDI-TOF MS, *m*/*z*: calcd for $C_{26}H_{32}N_2S_3$: 468.173, found: 468.631 $[M]^+$.

*4.2.3. 5-(7-(3-Thiophen-2-yl)benzo[c][1,2,5]thiadiazol-4-yl)thiophene-2-carbaldehyde (**3**).* This intermediate was prepared as described in a previous report.[20]

*4.2.4. 4-Hexyl-5-(7-(3-hexylthiophen-2-yl)benzo[c][1,2,5]thiadiazol-4-yl)thiophene-2-carbaldehyde (**4**).* This compound was prepared according to the synthetic procedure for **3**, using **2** instead of **1**.

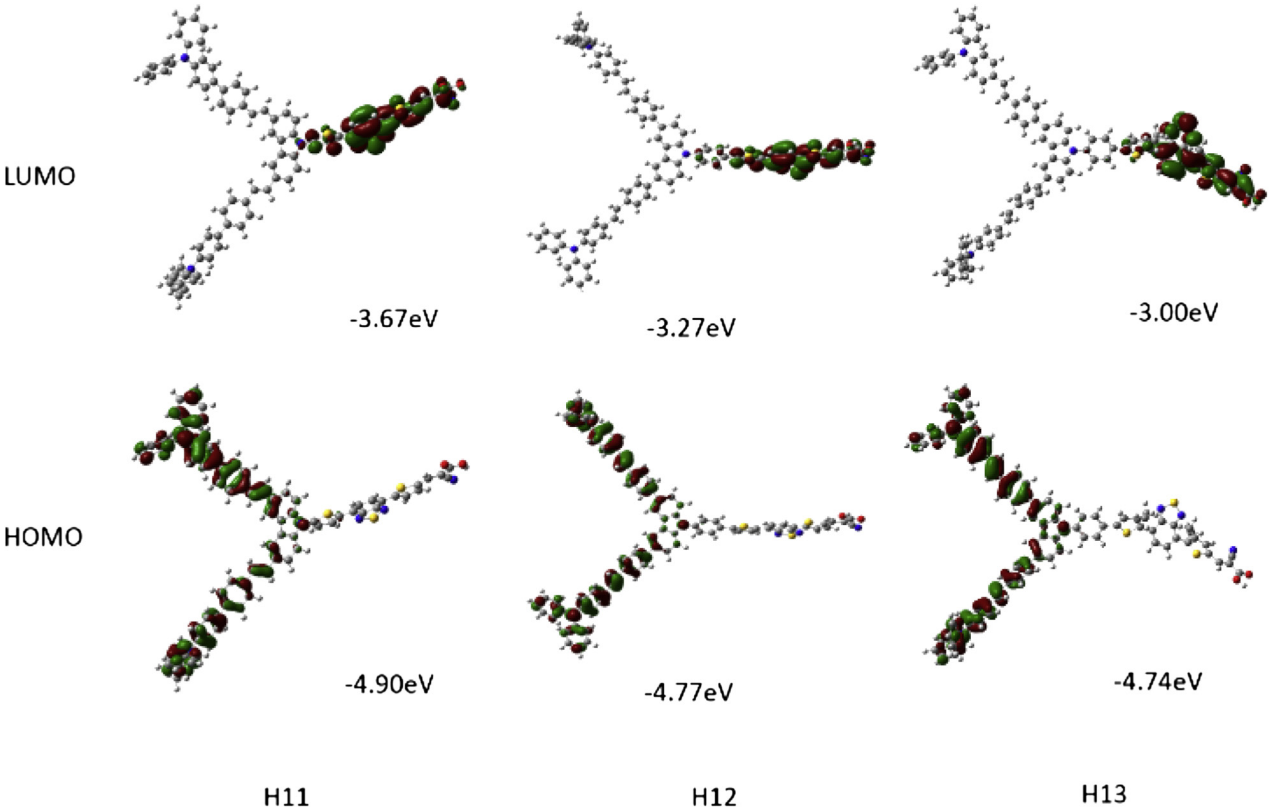

Fig. 2. Frontier molecular orbitals of **H11**–**H13**.

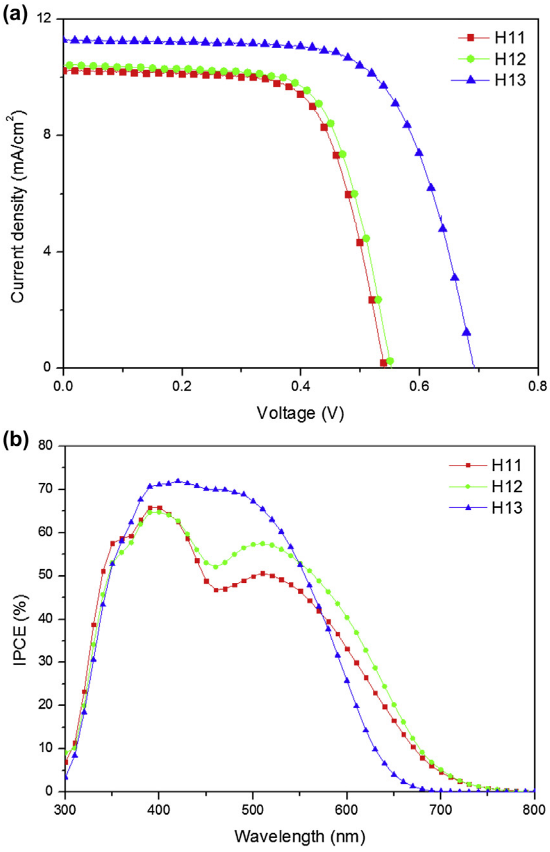

Fig. 3. (a) *J*–*V* curves and (b) IPCE spectra of **H11**–**H13**.

Table 2
Photovoltaic parameters of DSCs based on **H11**–**H13** in full sunlight (AM 1.5G, 100 mW cm^{-2})

Dye	V_{oc} (V)	J_{sc} (mA/cm^2)	FF	η (%)	Maximum efficiency
H11	0.54±0.00	9.14±1.18	0.67±0.01	3.32±0.47	3.79
H12	0.55±0.00	10.01±0.60	0.68±0.01	3.70±0.27	3.97
H13	0.70±0.02	11.11±0.59	0.66±0.02	5.11±0.16	5.27
H13[a]	0.72±0.01	12.07±0.60	0.72±0.01	6.19±0.13	6.32
N719	0.73±0.01	15.81±0.66	0.67±0.02	7.80±0.22	8.02

[a] The device was fabricated with 10 mM CDCA.

The product was obtained as an orange liquid (450 mg, 64%). ^{1}H NMR (300 MHz, DMSO-d_6): δ (ppm) 9.97 (s, 1H), 7.80 (s, 1H), 7.68–7.74 (m, 2H), 7.46–7.47 (d, J=4 Hz, 1H), 7.12–7.13 (d, J=4.3 Hz, 1H), 2.67–2.73 (m, 4H), 1.62–1.67 (m, 4H), 1.18–1.26 (m, 12H), 0.81–0.85 (t, J=6.2 Hz, 6H); ^{13}C (75 MHz, CDCl$_3$): δ (ppm) 182.9, 154.2, 135.6, 143.1, 142.9, 142.5, 142.1, 137.8, 131.8, 130.4, 129.6, 129.4, 129.1, 126.3, 125.9, 31.6, 31.5, 30.7, 30.4, 29.4, 29.3, 29.1, 29.0, 22.5, 22.4, 14.1, 14.0; MALDI-TOF MS, m/z: calcd for $C_{27}H_{32}N_2OS_3$: 496.168, found: 496.639 [M]$^+$.

*4.2.5. 5-(7-(5-Iodothiophen-2-yl)benzo[c][1,2,5]thiadiazol-4-yl)thiophene-2-carbaldehyde (**5**).*[19] *N*-Iodosuccinimide (NIS, 1.03 g, 4.57 mmol) was slowly added to a solution of **3** (500 mg, 1.52 mmol) in MC (30 mL) and acetic acid (30 mL) at room temperature, and the mixture was stirred overnight. After the reaction was complete, the mixture was filtered, and washed with water (590 mg, 91.4%). Mp 263–265 °C; ^{1}H NMR (300 MHz, DMSO-d_6): δ (ppm) 9.99 (s, 1H), 8.28–8.34 (m, 2H), 8.12–8.18 (m, 2H), 7.88–7.89 (d, J=3 Hz, 1H), 7.49–7.51 (d, J=6 Hz, 1H); ^{13}C NMR (150 MHz, DMSO-d_6): δ (ppm) 184.5, 151.7, 151.6, 147.0, 143.6, 138.1,

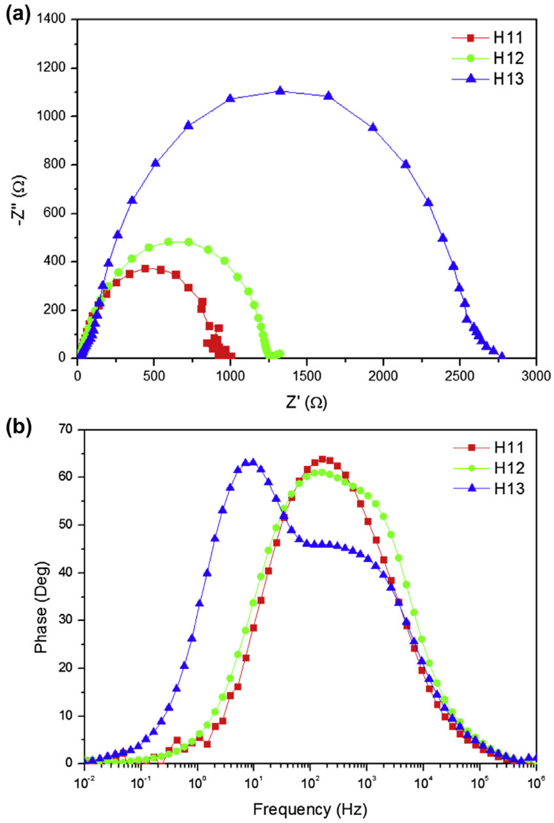

Fig. 4. (a) Nyquist plots and (b) Bode plots of **H11**–**H13**-sensitized solar cells under open-circuit.

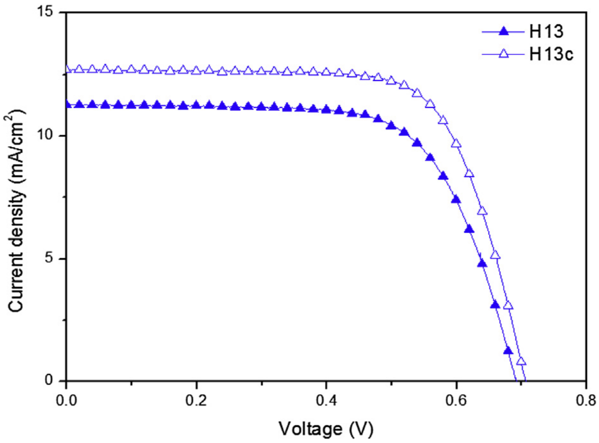

Fig. 5. *J*–*V* curve of **H13** and **H13** with CDCA based cell.

138.0, 129.2, 128.2, 128.0, 127.9, 127.0, 125.5, 123.5; MALDI-TOF MS, *m*/*z*: calcd for $C_{15}H_7IN_2OS_3$: 453.877, found: 454.189 $[M]^+$.

*4.2.6. 4-Hexyl-5-(7-(3-hexyl-5-iodothiophen-2-yl)benzo[c][1,2,5]thiadiazol-4-yl)thiophene-2-carbaldehyde (**6**).* This compound was prepared according to the synthetic procedure of **5**, using **4** instead of **3**. After the reaction, the mixture was extracted with MC and water, and the organic layer was dried over Na_2SO_4. The solvent was evaporated to give an orange liquid product (436 mg, 90%), which was purified by silica gel column chromatography (eluent; MC/Hex=1:1); ^{1}H NMR (300 MHz, $CDCl_3$): δ (ppm) 9.96 (s, 1H), 7.79 (s, 1H), 7.70–7.72 (d, *J*=7.3 Hz, 1H), 7.63–7.65 (d, *J*=7.3 Hz, 1H), 7.26 (s, 1H), 2.63–2.70 (m, 4H), 1.59–1.67 (m, 4H), 1.21–1.28 (m, 12H), 0.80–0.84 (t, *J*=6.5 Hz, 6H); ^{13}C (75 MHz, $CDCl_3$): δ (ppm) 182.9, 153.9, 153.5, 143.9, 143.2, 143.0, 142.3, 130.2, 129.4, 127.7, 126.4, 75.1, 31.5, 31.5, 30.6, 30.4, 29.3, 29.1, 29.0, 22.5, 22.5, 14.0, 14.0; MALDI-TOF MS, *m*/*z*: calcd for $C_{27}H_{31}IN_2OS_3$: 622.064, found: 622.646 $[M]^+$.

*4.2.7. 4,4′-(1E,1′E)-2,2′-(4,4′-(9H-Carbazole-3,6-diyl)bis(4,1-phenylene))bis(ethene-2,1-diyl)bis(N,N-diphenylaniline) (**7**).* This intermediate was prepared as described in a previous report.[21]

*4.2.8. 3,6-Bis-{4-[2-(4-diphenylamino-phenyl)-vinyl]-phenyl}-9-4-bromophenyl-carbazole (**8**).* A mixture of **7** (500 mg, 0.583 mmol), 1-bromo-4-iodobenzene (110 mg, 0.388 mmol), Cu powder (74 mg, 1.165 mmol), K_2CO_3 (215 mg, 1.554 mmol), and 18-crown-6 (103 mg, 0.388 mmol) in *o*-dichlorobenzene was refluxed for 36 h. After the reaction was complete, the mixture was poured into EtOH and the solid was filtered. The solvent was evaporated to give a pale yellow solid (240 mg, 61%), which was purified by silica gel column chromatography (eluent; ethyl acetate (EA)/Hex=1:30). Mp 196–198 °C; ^{1}H NMR (300 MHz, $CDCl_3$): δ (ppm) 8.44 (s, 2H), 7.72–7.78 (m, 8H), 7.62–7.65 (m, 4H), 7.52–7.55 (m, 2H), 7.43–7.49 (m, 6H), 7.32 (m, 4H), 7.03–7.16 (m, 24H); ^{13}C (75 MHz, $CDCl_3$): δ (ppm) 147.6, 147.4, 140.5, 136.2, 133.5, 133.2, 131.6, 129.3, 128.5, 128.0, 127.4, 127.3, 127.0, 126.8, 126.7, 125.6, 124.5, 124.2, 123.6, 123.0, 118.7, 110.0; MALDI-TOF MS, *m*/*z*: calcd for $C_{70}H_{50}BrN_3$: 1011.319, found: 1011.484 $[M]^+$.

*4.2.9. 3,6-Bis-{4-[2-(4-diphenylamino-phenyl)-vinyl]-phenyl}-9-4-(4,4,5,5-tetramethyl-1,3,2-dioxaborolan-2-yl)phenyl-carbazole (**9**).* A mixture of **8** (230 mg, 0.227 mmol), bis(pinacolato)diboron (144 mg, 0.567 mmol), $PdCl_2(dppf)\cdot CH_2Cl_2$ (37 mg, 0.045 mmol), and potassium acetate (89 mg, 0.908 mmol) in 1,4-dioxane (25 mL) was refluxed for 24 h. After the reaction was complete, the solvent was removed under high vacuum and the residue was extracted with MC and water. The solvent was evaporated to give a pale yellow solid (100 mg, 42%), which was purified by silica gel chromatography (eluent; MC/Hex=1:1). Mp 186–188 °C; ^{1}H NMR (300 MHz, $CDCl_3$): δ (ppm) 8.44 (s, 2H), 8.10–8.12 (d, *J*=7.9 Hz, 2H), 7.71–7.77 (t, *J*=8.8 Hz, 6H), 7.62–7.68 (t, *J*=9.1 Hz, 6H), 7.53–7.55 (d, *J*=8.5 Hz, 4H), 7.43–7.46 (d, *J*=8.5 Hz, 4H), 7.32 (s, 2H), 7.03–7.16 (m, 24H); ^{13}C (75 MHz, $CDCl_3$): δ (ppm) 147.6, 147.3, 140.7, 140.5, 136.5, 136.1, 133.3, 131.7, 129.3, 127.9, 127.4, 127.3, 126.8, 126.7, 125.9, 125.5, 124.5, 124.2, 123.7, 123.0, 118.6, 110.3, 84.1, 83.5, 25.0, 24.9; MALDI-TOF MS, *m*/*z*: calcd for $C_{76}H_{62}BN_3O_2$: 1059.494, found: 1059.564 $[M]^+$.

*4.2.10. 5-(7-(5-(3,6-Bis(4-(4-(diphenylamino)styryl)phenyl)-9H-carbazol-9-yl)thiophen-2-yl)benzo[c][1,2,5]thiadiazol-4-yl)thiophene-2-carbaldehyde (**10**).* A mixture of **7** (400 mg, 0.466 mmol), **5** (318 mg, 0.699 mmol), Cu powder (21 mg, 0.326 mmol), potassium acetate (258 mg, 1.864 mmol), and 18-crown-6 (37 mg, 0.139 mmol) in *o*-dichlorobenzene (45 mL) was refluxed for 48 h. After the reaction was complete, the solvent was removed by high vacuum, extracted with MC, and dried over sodium sulfate. The solvent was evaporated to give a reddish brown solid (416 mg, 75%), which was purified by silica gel chromatography (eluent; MC/Hex=2:1). Mp 194–197 °C; ^{1}H NMR (300 MHz, $CDCl_3$): δ (ppm) 9.92 (s, 1H), 8.26 (s, 2H), 8.09–8.03 (dd, *J*=3.7 Hz, 12.9 Hz, 2H), 7.78–7.71 (m, 2H), 7.64–7.53 (m, 13H), 7.42–7.40 (d, *J*=8.4 Hz, 4H), 7.31–7.26 (m, 6H), 7.21–7.13 (m, 10H), 7.08–7.01 (m, 13H); ^{13}C (75 MHz, $CDCl_3$): δ (ppm) 183.0, 158.2, 152.5, 147.6, 147.4, 141.4, 140.7, 140.4, 136.8, 136.3, 134.2, 131.6, 129.6, 129.3, 128.0, 127.5, 127.4, 126.8, 126.6, 126.0, 124.5, 123.6, 123.1, 118.6, 110.8; MALDI-TOF MS, *m*/*z*: calcd for $C_{79}H_{53}N_5OS_3$: 1183.341, found: 1183.199 $[M]^+$.

*4.2.11. 5-(7-(5-(4-(3,6-Bis(4-(4-(diphenylamino)styryl)phenyl)-9H-carbazol-9-yl)phenyl)thiophen-2-yl)benzo[c][1,2,5]thiadiazol-4-yl)thiophene-2-carbaldehyde (**11**).* This compound was prepared according to the same synthetic procedure as **2**, using **5** instead of 4,7-dibromobenzo[*c*][1,2,5]thiadiazole and **9** instead of 2-(3-hexylthiophen-2-yl)-4,4,5,5-tetramethyl-1,3,2-dioxaborolane. The product was obtained as a dark red solid (124 mg, 42%). Mp 252–254 °C; ^{1}H NMR (300 MHz, $CDCl_3$): δ (ppm) 10.00 (s, 1H), 8.46 (s, 3H), 8.26 (s, 2H), 7.98–8.05 (m, 6H), 7.88 (s, 2H), 7.65–7.70 (d, *J*=1.4 Hz, 5H), 7.59–7.62 (d, *J*=1.1 Hz, 5H), 7.43–7.60 (d, *J*=0.8 Hz, 6H), 7.06–7.16 (m, 27H); ^{13}C NMR (75 MHz, $CDCl_3$): δ (ppm) 183.0, 152.3, 147.6, 147.3, 140.5, 136.1, 133.3, 131.6, 129.6, 129.3, 127.9, 127.4, 127.3, 127.2, 126.8, 126.7, 124.9, 124.7, 124.5, 124.2, 123.6, 123.0, 118.6, 110.2; MALDI-TOF MS, *m*/*z*: calcd for $C_{85}H_{57}N_5OS_3$: 1259.373, found: 1259.394 [M]$^+$.

*4.2.12. 5-(7-(5-(4-(3,6-Bis(4-(4-(diphenylamino)styryl)phenyl)-9H-carbazol-9-yl)phenyl)-3-hexylthiophen-2-yl)benzo[c][1,2,5]thiadiazol-4-yl)-4-hexylthiophene-2-carbaldehyde (**12**).* This compound was prepared according to the same synthetic procedure as **2**, using **6** instead of 4,7-dibromobenzo[*c*][1,2,5]thiadiazole and **9** instead of 2-(3-hexylthiophen-2-yl)-4,4,5,5-tetramethyl-1,3,2-dioxaborolane. The product was obtained as an orange solid (70 mg, 52%). Mp 197–199 °C; ^{1}H NMR (300 MHz, $CDCl_3$): δ (ppm) 9.99 (s, 1H), 7.94–7.97 (d, *J*=8.2 Hz, 2H), 7.74–7.78 (m, 8H), 7.63–7.70 (m, 8H), 7.55–7.58 (d, *J*=8.6 Hz, 2H), 7.44–7.48 (m, 4H), 7.30–7.32 (m, 4H), 6.99–7.19 (m, 24H), 2.69–2.81 (m, 4H), 1.63–1.78 (m, 4H), 1.25–1.28 (m, 12H), 0.86–0.90 (m, 6H); ^{13}C NMR (75 MHz, $CDCl_3$): δ (ppm) 183.0, 153.6, 147.6, 147.3, 143.2, 140.6, 137.8, 136.1, 133.3, 131.6, 130.4, 129.3, 127.9, 127.4, 127.2, 126.9, 126.7, 126.1, 125.6, 124.5, 124.2, 123.7, 123.0, 118.6, 110.3, 31.6, 31.5, 30.7, 30.4, 29.7, 29.4, 29.2, 29.0, 22.6, 22.5, 14.1; MALDI-TOF MS, *m*/*z*: calcd for $C_{97}H_{81}N_5OS_3$: 1427.560, found: 1427.679 [M]$^+$.

*4.2.13. (E)-3-(5-(7-(5-(3,6-Bis(4-(4-(diphenylamino)styryl)phenyl)-9H-carbazol-9-yl)thiophen-2-yl)benzo[c][1,2,5]thiadiazol-4-yl)thiophen-2-yl)-2-cyanoacrylic acid (**H11**).* Piperidine (51 μL, 0.51 mmol) was added to a mixture of **10** (200 mg, 0.17 mmol) and cyanoacetic acid (43 mg, 0.51 mmol) in acetonitrile (20 mL) and THF (20 mL). The mixture was refluxed overnight and then cooled to room temperature. The mixture was extracted with MC and water, and the organic phase was dried over sodium sulfate. The solvent was evaporated to give a dark brown solid (98 mg, 46%), which was purified by silica gel chromatography (eluent; MC/MeOH/triethylamine (TEA)=10:1:0.1). Mp 208–211 °C; ^{1}H NMR (300 MHz, DMSO-d_6): δ (ppm) 9.36 (s, 1H), 8.82 (s, 1H), 8.38–8.29 (m, 4H), 7.94–7.92 (m, 2H), 7.89–7.86 (d, *J*=8.5 Hz, 5H), 7.73–7.67 (m, 6H), 7.57–7.55 (d, *J*=7.9 Hz, 3H), 7.36–7.23 (m, 14H), 7.17–7.04 (m, 13H), 6.99–6.96 (d, *J*=8.1 Hz, 5H); ^{13}C NMR (75 MHz, DMSO-d_6): δ (ppm) 150.8, 147.5, 147.4, 132.1, 130.1, 128.2, 127.4, 124.7, 123.8; HRMS, *m*/*z*: calcd for $C_{82}H_{54}N_6O_2S_3$: 1250.3470, found: 1250.3466.

*4.2.14. 3-(5-(7-(5-(4-(3,6-Bis(4-(4-(diphenylamino)styryl)phenyl)-9H-carbazol-9-yl)phenyl)thiophen-2-yl)benzo[c][1,2,5]thiadiazol-4-yl)thiophen-2-yl)-2-cyanoacrylic acid (**H12**).* This compound was prepared according to the same synthetic procedure as **H11**, using **11** instead of **10**. The product was obtained as a dark red solid (55 mg, 48%). Mp 317–319 °C; ^{1}H NMR (300 MHz, $CDCl_3$): δ (ppm) 8.76 (s, 2H), 8.19–8.22 (m, 3H), 8.08–8.11 (m, 3H), 7.83–7.85 (m, 4H), 7.69–7.71 (d, *J*=7.8 Hz, 4H), 7.53–7.56 (m, 6H), 7.30–7.35 (m, 10H), 7.21–7.25 (m, 4H), 6.95–7.09 (m, 20H); ^{13}C NMR (150 MHz, $CDCl_3$): δ (ppm) 147.6, 135.7, 129.3, 127.4, 124.4, 122.9; HRMS, *m*/*z*: calcd for $C_{88}H_{58}N_6O_2S_3$: 1326.3785, found: 1326.3783.

*4.2.15. 3-(5-(7-(5-(4-(3,6-Bis(4-(4-(diphenylamino)styryl)phenyl)-9H-carbazol-9-yl)phenyl)-3-hexylthiophen-2-yl)benzo[c][1,2,5]thiadiazol-4-yl)-4-hexylthiophen-2-yl)-2-cyanoacrylic acid (**H13**).* This compound was prepared according to the same synthetic procedure as **H11**, using **12** instead of **10**. The product was obtained as an orange solid (80 mg, 77%). Mp 299–302 °C; ^{1}H NMR (300 MHz, DMSO-d_6): δ (ppm) 8.77 (s, 2H), 8.12 (s, 1H), 8.02–8.05 (d, *J*=8 Hz, 2H), 7.81–7.87 (m, 8H), 7.68–7.76 (m, 8H), 7.53–7.56 (d, *J*=8.56 Hz, 6H), 7.30–7.35 (t, *J*=7.8 Hz, 8H), 7.24–7.26 (d, *J*=6.5 Hz, 2H), 6.96–7.10 (m, 18H), 2.63–2.73 (m, 4H), 1.49–1.65 (m, 4H), 1.11–1.15 (m, 12H), 0.72–0.76 (m, 6H); ^{13}C NMR (150 MHz, $CDCl_3$): δ (ppm) 153.7, 147.5, 147.2, 143.8, 143.3, 140.4, 136.8, 135.9, 133.0, 131.6, 129.7, 129.3, 127.7, 127.4, 126.8, 126.3, 125.1, 124.5, 124.1, 123.6, 123.0, 118.4, 115.2, 113.8, 110.0, 31.6, 31.4, 29.9, 29.3, 22.6, 14.1; HRMS, *m*/*z*: calcd for $C_{100}H_{82}N_6O_2S_3$: 1494.5664, found: 1494.5661.

4.3. Device fabrication

Fluorine-doped tin oxide (FTO) glass plates (Pilkington, 8 Ω sq^{-1}, 2.3 mm thick) were cleaned in a detergent solution in an ultrasonic bath for 15 min, and then rinsed with water and EtOH. The washed FTO glass plates were immersed in aqueous 10 mM $TiCl_4$ at 70 °C for 30 min. A transparent nanocrystalline layer was deposited on the FTO glass by the doctor blade printing method using TiO_2 paste (Solaronix, Ti–Nanoxide T/SP, and ENB Korea, TTP-20N) and a scattering layer paste (Dyesol Timo, 18NR-AO, Batch 314). The TiO_2 layer was gradually sintered according to a programmed procedure. The sintered layers (0.2 cm^2) consisted of a transparent layer (12 μm thick) and a scattering layer (10 μm thick). The TiO_2 electrodes were again treated with 10 mM $TiCl_4$ at 70 °C for 30 min and sintered at 450 °C. Subsequently, the TiO_2 electrodes were immersed in solutions of the dyes (0.3 mM in THF/EtOH (2:1)) at 50 °C for 8 h in the dark. The FTO plates for the counter electrodes were cleaned in a detergent solution in an ultrasonic bath for 15 min. Then, the counter electrodes were prepared by coating each FTO plate with a drop of H_2PtCl_6 solution (2 mg Pt in 1 mL EtOH) and heating the plate to 450 °C, causing the dyes adsorbed on the TiO_2 electrode to adhere to the counter electrode by coverage with a hot-melt polymer film (Solaronix, Meltonix 1170-60). A drop of electrolyte solution was injected through a hole in the counter electrode and driven into the cell. Finally, the hole was sealed using the hot-melt polymer film and a cover glass (0.1 mm thick).

Acknowledgements

This work was supported by the National Research Foundation of Korea (NRF) grant funded by the Korea government (MSIP) for the Center for Next Generation Dye-sensitized Solar Cells (No. 2013004800), and by a grant from the New & Renewable Energy Technology Development Program of the KETEP (No. 20113020010070), funded by the Ministry of Knowledge Economy.

References and notes

1. O'Regan, B.; Grätzel, M. *Nature* **1991**, *353*, 737.
2. (a) Nazeeruddin, M. K.; Kay, A.; Rodicio, L.; Humphry-Baker, R.; Müller, E.; Liska, P.; Vlachopoulos, N.; Grätzel, M. *J. Am. Chem. Soc.* **1993**, *115*, 6382; (b) Nazeeruddin, M. K.; Zakeeruddin, S. M.; Humphry-Baker, R.; Jirousek, M.; Liska, P.; Vlachopoulos, N.; Grätzel, M. *Inorg. Chem.* **1999**, *38*, 6298; (c) Nazeeruddin, M. K.; Pechy, P.; Renouard, T.; Zakeeruddin, S. M.; Humphry-Baker, R.; Comte, P.; Liska, P.; Cevey, L.; Costa, E.; Shklover, V.; Spiccia, L.; Deacon, G. B.; Bignozzi, C. A.; Grätzel, M. *J. Am. Chem. Soc.* **2001**, *123*, 1613; (d) Gao, F.; Wang, Y.; Shi, D.; Zhang, J.; Wang, M.; Jing, X.; Humphry-Baker, R.; Wang, P.; Zakeeruddin, S. M.; Grätzel, M. *J. Am. Chem. Soc.* **2008**, *130*, 10720.
3. Fischer, M. K. R.; Wenger, S.; Wang, M.; Mishra, A.; Zakeeruddin, S. M.; Grätzel, M.; Bäuerle, P. *Chem. Mater.* **2010**, *22*, 1836.
4. (a) Zeng, W.; Cao, Y.; Bai, Y.; Wang, Y.; Shi, Y.; Zhang, M.; Wang, F.; Pan, C.; Wang, P. *Chem. Mater.* **2010**, *22*, 1915; (b) Kim, J.; Jo, Y.; Choi, W.-Y.; Jun, Y.; Yang, C. *Tetrahedron Lett.* **2011**, *52*, 2764.
5. Yella, A.; Lee, H.-W.; Tsao, H. N.; Yi, C.; Chandiran, A. K.; Nazeeruddin, M. K.; Diau, E. W.-G.; Yeh, C.-Y.; Zakeeruddin, S. M.; Grätzel, M. *Science* **2011**, *334*, 629.

6. (a) Argazzi, R.; Bignozzi, C. A.; Heimer, T. A.; Castellano, F. N.; Meyer, G. J. *J. Am. Chem. Soc.* **1995**, *117*, 11815; (b) Haque, S. A.; Handa, S.; Peter, K.; Palomares, E.; Thelakkat, M.; Durrant, J. R. *Angew. Chem., Int. Ed.* **2005**, *44*, 5740.
7. Wu, Y.; Zhu, W. *Chem. Soc. Rev.* **2013**, *42*, 2039.
8. Mishra, A.; Fischer, M. K. R.; Bäuerle, P. *Angew. Chem., Int. Ed.* **2009**, *48*, 2474.
9. Wu, Y.; Zhang, X.; Li, W.; Wang, Z.-S.; Tian, H.; Zhu, W. *Adv. Energy Mater.* **2012**, *2*, 149.
10. (a) Choi, H.; Baik, C.; Kang, S. O.; Ko, J.; Kang, M.-S.; Nazeeruddin, M. K.; Grätzel, M. *Angew. Chem., Int. Ed.* **2008**, *47*, 327; (b) Hwang, S.; Lee, J. H.; Park, C.; Lee, H.; Kim, C.; Park, C.; Lee, M.-H.; Lee, W.; Park, J.; Kim, K.; Park, N.-G.; Kim, C. *Chem. Commun.* **2007**, 4887; (c) Wang, Z. S.; Koumura, N.; Cui, Y.; Takahashi, M.; Sekiguchi, H.; Mori, A.; Kubo, T.; Furube, A.; Hara, K. *Chem. Mater.* **2008**, *20*, 3993; (d) Ning, Z. J.; Zhang, Q.; Wu, W. J.; Pei, H. C.; Liu, B.; Tian, H. *J. Org. Chem.* **2008**, *73*, 3791.
11. (a) Thomas, K. R. J.; Lin, J. T.; Velusamy, M.; Tao, Y. T.; Chuen, C. H. *Adv. Funct. Mater.* **2004**, *14*, 83; (b) Raimundo, J.; Blanchard, P.; Brisset, H.; Akoudad, S.; Roncali, J. *Chem. Commun.* **2000**, 939; (c) Velusamy, M.; Thomas, K. R. J.; Lin, J. T.; Hsu, Y. C.; Ho, K. C. *Org. Lett.* **2005**, *7*, 1899.
12. (a) Cui, Y.; Wu, Y. Z.; Lu, X. F.; Zhang, X.; Zhou, G.; Miapeh, F. B.; Zhu, W. H.; Wang, Z. S. *Chem. Mater.* **2011**, *23*, 4394; (b) Mao, J. Y.; Guo, F. L.; Ying, W. J.; Wu, W. J.; Li, J.; Hua, J. L. *Chem.—Asian J.* **2012**, *7*, 982; (c) Uemura, Y.; Mori, S.; Hara, K.; Koumura, N. *Chem. Lett.* **2011**, *40*, 872.
13. (a) Chang, D. W.; Lee, H. J.; Kim, J. H.; Park, S. Y.; Park, S. M.; Dai, L.; Baek, J. B. *Org. Lett.* **2011**, *13*, 3880; (b) Pei, K.; Wu, Y. Z.; Wu, W. J.; Zhang, Q.; Chen, B. Q.; Tian, H.; Zhu, W. H. *Chem.—Eur. J.* **2012**, *18*, 8190; (c) Lu, X. F.; Feng, Q. Y.; Lan, T.; Zhou, G.; Wang, Z.-S. *Chem. Mater.* **2012**, *24*, 3179; (d) Shi, J.; Chen, J. N.; Chai, Z. F.; Wang, H.; Tang, R. L.; Fan, K.; Wu, M.; Han, H. W.; Qin, J. G.; Peng, T. Y.; Li, Q. Q.; Li, Z. *J. Mater. Chem.* **2012**, *22*, 18830.
14. (a) Qu, S. Y.; Wu, W. J.; Hua, J. L.; Kong, C.; Long, Y. T.; Tian, H. *J. Phys. Chem. C* **2010**, *114*, 1343; (b) Qu, S. Y.; Wang, B.; Guo, F. L.; Li, J.; Wu, W. J.; Kong, C.; Long, Y. T.; Hua, J. L. *Dyes Pigm.* **2012**, *92*, 1384.
15. Kim, B.; Yeom, H. R.; Choi, W.-Y.; Kim, J. Y.; Yang, C. *Tetrahedron* **2012**, *68*, 6696.
16. Ismael, L.-D.; Mingkui, W.; Humphry-Baker, R.; Mine Ince, M.; Victoria, M.-D.; Nazeeruddin, M. K.; Tomás, T.; Grätzel, M. *Angew. Chem., Int. Ed.* **2012**, *51*, 1895.
17. Mao, J.; He, N.; Ning, Z.; Zhang, Q.; Guo, F.; Chen, L.; Wu, W.; Hua, J.; Tian, H. *Angew. Chem., Int. Ed.* **2012**, *51*, 1.
18. (a) Hara, K.; Kurashige, M.; Ito, S.; Shinpo, A.; Suga, S.; Sayama, K.; Arakawa, H. *Chem. Commun.* **2003**, 252; (b) Li, S. L.; Jiang, K. J.; Shao, K. F.; Yang, L. M. *Chem. Commun.* **2006**, 2792; (c) Chen, R.; Yang, X.; Tian, H.; Wang, X.; Hagfeldt, A.; Sun, L. *Chem. Mater.* **2007**, *19*, 4007; (d) Thomas, K. R. J.; Hsu, Y. C.; Lin, J. T.; Lee, K. M.; Ho, K. C.; Lai, C. H.; Cheng, Y. M.; Chou, P. T. *Chem. Mater.* **2008**, *20*, 1830.
19. Lee, D. H.; Lee, M. J.; Song, H. M.; Song, B. J.; Seo, K. D.; Pastore, M.; Anselmi, C.; Fantacci, S.; Angelis, F. D.; Nazeeruddin, M. K.; Gräetzel, M.; Kim, H. K. *Dyes Pigm.* **2011**, *91*, 192.
20. Zeng, T.-W.; Ho, C.-C.; Tu, Y.-C.; Tu, G.-Y.; Wang, L.-Y.; Su, W.-F. *Langmuir* **2011**, *27*, 15255.
21. Lee, W.; Cho, N.; Kwon, J.; Ko, J.; Hong, J.-I. *Chem.—Asian J.* **2012**, *7*, 343.
22. Teng, C.; Yang, X.; Yang, C.; Li, S.; Cheng, M.; Hagfeldt, A.; Sun, L. *J. Phys. Chem. C* **2010**, *114*, 9101.
23. Boschloo, G.; Hagfeldt, A. *Acc. Chem. Res.* **2009**, *42*, 1819.
24. (a) Zhu, W.; Wu, Y.; Wang, S.; Li, W.; Li, X.; Chen, J.; Wang, Z.-s; Tian, H. *Adv. Funct. Mater.* **2011**, *21*, 756; (b) Haid, S.; Marszalek, M.; Mishra, A.; Wielopolski, M.; Teuscher, J.; Moser, J.-E.; Humphry-Baker, R.; Zakeeruddin, S. M.; Grätzel, M.; Bäuerle, P. *Adv. Funct. Mater.* **2012**, *22*, 1291.
25. (a) Lin, L.-Y.; Tsai, C.-H.; Wong, K.-T.; Tsai, A.-I. *J. Org. Chem.* **2010**, *75*, 4778; (b) Velusamy, M.; Hsu, Y.-C.; Lin, J. T.; Chang, C.-W.; Hsu, C.-P. *Chem.—Asian J.* **2010**, *5*, 87.
26. Kern, R.; Sastrawan, R.; Ferber, J.; Stangl, R.; Luther, J. *Electrochim. Acta* **2002**, *47*, 4213.
27. (a) Berger, T.; Anta, J. A.; Morales-Florez, V. *J. Phys. Chem. C* **2012**, *116*, 11444; (b) Ardo, S.; Meyer, G. J. *Chem. Soc. Rev.* **2009**, *38*, 115.
28. Ning, Z.; Zhang, Q.; Pei, H.; Luan, J.; Lu, C.; Cui, Y.; Tian, H. *J. Phys. Chem. C* **2009**, *113*, 10307.
29. Kim, J.-J.; Choi, H.; Lee, J. W.; Kang, M. S.; Song, K.; Kang, S. O.; Ko, J. *J. Mater. Chem.* **2008**, *18*, 5223.